Reconstructed adiabatic potential energy surfaces for self-trapped excitons in binary oxides

1990 J. Phys.: Condens. Matter 2 10021

(http://iopscience.iop.org/0953-8984/2/50/006)

J. Phys.: Condens. Matter **2** (1990) 10021–10032. Printed in the UK

Reconstructed adiabatic potential energy surfaces for self-trapped excitons in binary oxides

M Georgiev† and N Itoh

Department of Physics, Faculty of Science, Nagoya University, Furo-cho, Chikusa-ku, Nagoya 464-01, Japan

Received 25 May 1990

Abstract. Adiabatic potential energy surfaces (APESs) for self-trapped excitons (STEs) (incipient Frenkel pairs) in α-quartz and α-alumina are deduced from experimental temperature dependences of the decay constants for transient volume change, optical absorption and luminescence, associated with the lowest STE state, as induced by an electron pulse irradiation. APES profiles along some effective 'reactive coordinate' are obtained by processing the temperature data by means of the reaction rate method. The resulting profiles suggest that STEs and defect pairs (DPs) in α-quartz, each incorporating an interstitial oxygen (O_i^-) and a singly charged oxygen vacancy (E_1' centre), are likely to form as two energetically non-equivalent pseudo-Jahn–Teller distortions of the quasi-symmetry of the saddle-point configuration between STEs and DPs. The APES for α-alumina appears to be inherently different from that for α-quartz. Now the pseudo-Jahn–Teller conjecture is not likely to apply immediately, owing to a very small crossover splitting. Implications for the defect formation process in quartz will be discussed.

1. Introduction

Self-trapped excitons (STEs) in binary oxides are of considerable fundamental interest, since on the one hand these are strongly coupled electron–phonon systems incorporating large lattice distortions and on the other hand they can be regarded as incipient defect pairs (DPs), precursors to stable defect formation under ionizing radiation [1]. One of the key questions is just what is the shape of the adiabatic potential energy surface (APES) that controls the conversion from incipient to distant DPs, and what, in a broader sense, is the driving force of that conversion.

Recent experiments on the transient volume change associated with the lowest-energy state of STEs, produced by irradiation with an electronic pulse, seem to provide a clue to the answer [2, 3]. The temperature dependence of the decay constant has been measured in samples of α-SiO_2 and α-Al_2O_3 and in both cases found to consist of a lower-temperature portion where the lifetime is virtually temperature independent, followed by a thermally activated branch at higher temperatures. Nevertheless, an essential difference becomes obvious even at first glance: the transition from low- to high-temperature branches occurs more gradually in Al_2O_3 than it does in SiO_2. In SiO_2

† On leave of absence from the Institute of Solid State Physics, Bulgarian Academy of Sciences, Sofia, Bulgaria.

0953-8984/90/5010021 + 12 $03.50

the decay constants of a 2.8 eV luminescence and a 5.8 eV absorption both starting from the same STE state coincide nicely with the temperature curve of the volume change.

Physically the volume change occurs because of the lattice distortion associated with the self-trapping. Its decay is due to radiative and non-radiative transitions to a ground electron–hole state [4]. Of these, the latter transitions are immediately sensitive to the shape of the vibronic potential energy surface and could in fact give information about that surface if extracted from the overall decay rate. The total lifetime reads

$$\tau(T) = 1/[1/\tau_0 + k_{if}(T)] \tag{1}$$

where τ_0 is the radiative lifetime, while k_{if} is the non-radiative de-excitation rate. While the former is rather long and is usually believed to be temperature independent, the latter is largely responsible for the thermally activated branch of a $\tau(T)$ curve.

The present paper describes what we believe to be a first attempt to interpret the non-radiative lifetime data quantum mechanically in terms of an appropriate rate process. Fitting to the experimental temperature data then leads to a reconstruction of the APES profile, controlling that rate along the corresponding reactive coordinate.

2. Non-radiative rate

An early interpretation of k_{if} as a classical rate $\nu \exp(-E/k_B T)$ has been reported elsewhere [3]. The frequency factors and the activation energies derived from fitting to the experimental data are $\nu = 1.1 \times 10^{14}\,s^{-1}$ and $E = 0.40$ eV for SiO_2, and $\nu = 5.9 \times 10^4\,s^{-1}$ and $E = 0.13$ eV for Al_2O_3. The radiative lifetimes used for the above estimates are $\tau_0 = 10^{-3}$ s for SiO_2 and $\tau_0 = 1.2 \times 10^{-2}$ s for Al_2O_3. Striking features of the classical analysis are the numerical values of the frequency factor which is slightly too high (0.45 eV) for SiO_2 and much too low for Al_2O_3. High pre-exponential factors can be indicative of a considerable tunnelling contribution through the crossover barrier, while low frequency factors can arise from non-adiabatic electron transfer. In both cases the simple classical description does not apply.

A quantum mechanical rate theory accounting for both adiabaticity and tunnelling has been described elsewhere [5]. The rate is obtained as a sum of products $W_{el}(E_n)W_{conf}(E_n)$ over the various vibronic energy levels E_n of the weighted probabilities of a change in the electronic state and of configurational tunnelling respectively. The former accounts for the adiabaticity, while the latter for the tunnelling across the barrier. Thermal equilibrium in the initial electronic state i is required. In a simple case of harmonic motion along a 'reactive-mode coordinate',

$$k_{if} = 2\nu \sinh\left(\frac{h\nu}{2k_B T}\right) \sum_{n=0} W_{el}(E_n)W_{conf}(E_n) \exp\left(-\frac{E_n}{k_B T}\right) \tag{2}$$

where ν is the bare-mode frequency. Expressions for $W_{el}(E_n)$ and $W_{conf}(E_n)$ are readily available for electronic transitions coupled either strongly or weakly to the promoting phonon mode. Both quantum mechanical and quasi-classical approaches to the transition probabilities have been applied, leading to convergent results [5].

Specifying the nature of the underlying non-radiative process, it is conceivable that the STE would make an attempt to convert into a DP before de-excitation to the ground (electronic) state (GS). In fact the DP-to-GS de-excitation channel should be rather efficient, since no stable defect production has been observed in α-quartz under electron

irradiation. If so, the STE-to-DP part may be expected to be rate determining for the non-radiative process in (1). Following the commonly accepted viewpoint, we assume that the electronic transition from STE to DP couples strongly to the promoting vibration [4]. For reasons to be specified below, this STE-to-DP phonon-coupled process may also be expected to be exothermic.

Now the vibronic transitions from the initial electronic state (STE) will start from the lowest level E_0. For such transitions the theory predicts [6]

$$W_{\text{conf}}(E_0) = \pi(F_{0m}^2/2^m m!)\exp(-Q^2/E_r h\nu - E_r/h\nu) \tag{3}$$

where

$$F_{0m} = \xi_0 H_m(\xi_c - \xi_0) + 2mH_{m-1}(\xi_c - \xi_0).$$

m is the number of the corresponding quantized vibronic energy level, $E_m = E_0$ in the final electronic state (DP), $H_m(\ )$ are Hermite polynomials, ξ is the dimensionless phonon coordinate (which equals ξ_0 at the equilibrium DP configuration, and ξ_c at the STE–DP crossover), Q is the zero-point reaction heat, E_r is the lattice reorganization (relaxation) energy defined by

$$E_r = (K/2)(\Delta q)^2$$

where Δq is the interwell separation along q. This is the elastic energy expended to displace two parabolic wells of the same curvature at a distance Δq from each other.

For subbarrier transitions starting from higher vibronic levels at $n \geqslant 1$, quasi-classical techniques can be applied, leading to

$$W_{\text{conf}}(E_n) = 1/\{1 + \exp[P(E_n)]\} \tag{4}$$

where the phase integral is

$$P(E_n) = \frac{2}{h\nu}\sqrt{2K}\int_{q_l(E_n)}^{q_r(E_n)} \sqrt{E_L(q) - E_n}\,\mathrm{d}q. \tag{5}$$

Here $E_L(q)$ is the APES profile along the reactive coordinate $q = \sqrt{h\nu/K}\xi$, K is the mode spring constant, while $q_l(E_n)$ and $q_r(E_n)$ are the classical turning points at the barrier along q. For overbarrier transitions a reflective rule applies as a useful approximation:

$$W_{\text{conf}}(E_n) = 1/\{1 + \exp[-P(E_n)]\}. \tag{6}$$

Another quasi-classical formula has been worked out for adiabatic overbarrier transitions based on approximating the barrier top by an inverted parabola [5]:

$$E_L(q) = E_b + K_p(q - q_c)^2.$$

We next define Christov's [5] characteristic temperature as [7]

$$T_C = -h\nu(K_p/K)/\pi k_B. \tag{7}$$

Introducing T_c, one obtains a quasi-classical tunnelling probability

$$W_{\text{conf}}(E_n) = 1/\{1 + \exp[-2(E_n - E_b)/k_B T_c]\}. \tag{8}$$

In general, Christov's quasi-classical characteristics divide the entire temperature scale into ranges of

(i) subbarrier tunnelling ($T < T_c/2$),

(ii) 'thermally activated tunnelling' near the barrier top ($T_c/2 < T < 2T_c$) and
(iii) classical overbarrier jumps ($2T_c < T$),

leading to useful approximations for the rate.

The electron transfer probability $W_{el}(E_n)$ has been calculated following the Landau–Zener quasi-classical method [6]. Introducing the parameter

$$\gamma(E_n) = (V_{if}^2/2h\nu)/\sqrt{E_r|E_c - E_n|} \tag{9}$$

we get

$$W_{el}(E_n) = 2\gamma_n^{2(\gamma-1)}/[\Gamma(\gamma_n)]^2 \tag{10}$$

for subbarrier levels ($E_n < E_b$), and

$$W_{el}(E_n) = 2[1 - \exp(-2\pi\gamma_n)]/[2 - \exp(-2\pi\gamma_n)] \tag{11}$$

for overbarrier levels ($E_n > E_b$). Here

$$E_c = (E_r + Q)^2/4E_r \tag{12}$$

is the crossover energy, as measured from the bottom of the STE well, while $2V_{if}$ is the crossover adiabatic energy splitting. The crossover barrier height is $E_b = E_c - V_{if}$. Strictly speaking, equations (9) and (10) are more accurate for smaller gap energies ($V_{if} \ll E_c$).

The reaction rate method thus operates with four independent parameters, e.g. $h\nu$, V_{if}, E_b and Q, which can be extracted through fitting the rate (2) to experimental reciprocal-lifetime data. As the number of parameters obtainable by classical processing of the data is limited to two, it is clear that quantum mechanical rate processing can yield further information on the APES. Even though fitting by four parameters introduces some ambiguity in uniqueness, the best-fit values can rather be sorted out on physical grounds, as will be shown later.

3. Pseudo-Jahn–Teller effect

Vibronic interactions, such as the phonon-induced mixing of electronic states, are known to incite gross configurational transfigurements in crystalline solids [6]. Among these, the symmetry-breaking small pseudo-Jahn–Teller effect (PJTE) of mixing nearly degenerate electronic states seems to be a fairly general occurrence in exciton relaxation processes as demonstrated for conversion from on-centre to off-centre STEs [8] in alkali halides. We discuss first whether the same conjecture can be applied for the STE-to-DP conversion in a wide range of non-metallic solids.

The STE-to-DP conversion may require motion of an interstitial atom or ion, leaving a vacancy behind, over a barrier on the lowest APES. The PJTE conjecture may be applicable, if an excited state coupled with the lowest excited state through the translational anion motion from STE to DP has an APES minimum near (or at) the intermediate configuration, where the lowest APES takes a maximum. A few possible cases emerge where such an intermediate configuration exists, even though it does not occur in general. Thus it is one of the main goals of the present investigation to explore the applicability of the PJTE conjecture to the APES controlling the conversion from STE to DP in oxides. We show finally in the present paper that the intermediate state of the type described above exists for SiO_2, but not for Al_2O_3.

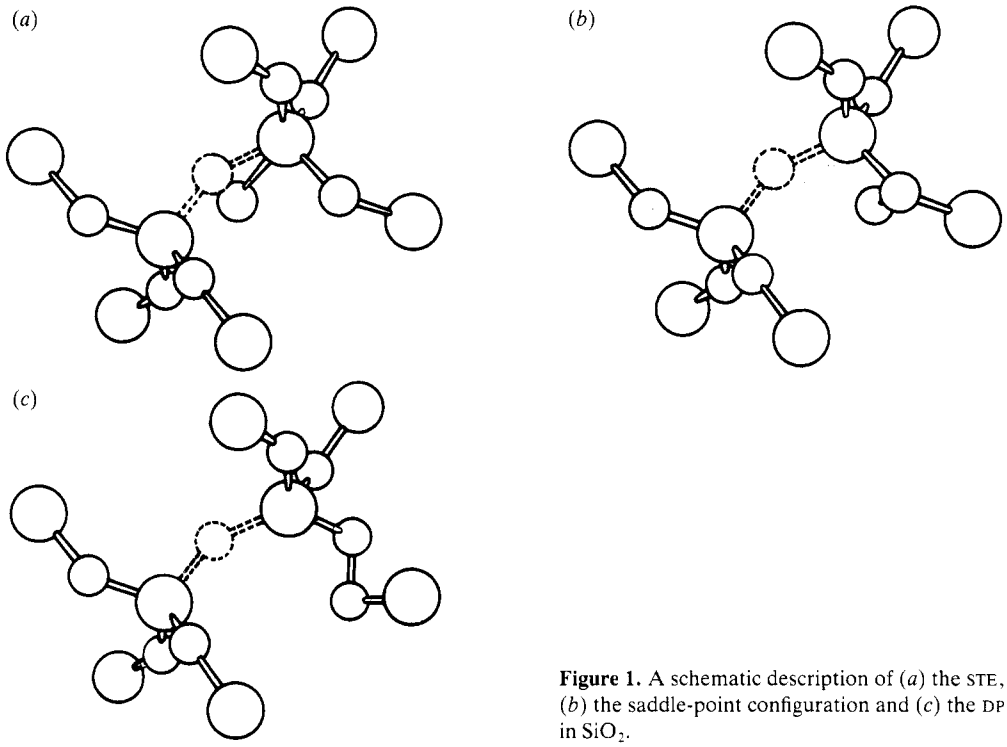

Figure 1. A schematic description of (*a*) the STE, (*b*) the saddle-point configuration and (*c*) the DP in SiO_2.

It is assumed for alkali halides in particular that the STE and DP comprising a Frenkel pair in the halogen sublattice constitute two neighbouring minima of the lowest-excited-state APES. Both the STE and the DP configurations include an X_2^- molecular ion (X denotes a halogen atom) and the STE-to-DP conversion involves migration of the interstitial X through a replacement reaction $X^- + X_2^- \rightarrow X_2^- + X^-$. It follows that the saddle-point configuration is most probably a linear X_3^{2-} molecular ion. Since the energy separation between X–X bonding and anti-bonding orbitals decreases as another X^- approaches an X_2^- ion, the X_3^{2-} can be regarded as an intermediate configuration at which the PJTE is effective.

Assignment of the intermediate configuration for SiO_2 is not straightforward according to a recent cluster calculation; a small oxygen displacement nearly perpendicular to the Si–O–Si bonds would lead to self-trapping of an exciton at a configuration shown in figure 1(*a*) [9]. The triplet spin multiplicity of the electron located on the neighbouring Si orbitals and the hole localized on the displaced oxygen explains both the large values of τ_0 and the zero-field splitting parameter, as obtained experimentally. Shluger and Stefanovich [10] have extended the calculation to larger oxygen separation in β-cristobalite. According to their calculation the DP appears to be composed of an oxygen vacancy at the O(1) site (figure 1(*c*)), while the O(1) ion has been rotated to intervene in one of the neighbouring Si–O bonds resulting in a Si–O–O bond. The atomic structure of the intermediate state may appear at an overcoordinated configuration, e.g. such as shown in figure 1(*b*). Since migration of O^- is involved in the STE-to-DP transformation, overcoordination will reduce the bonding strength and hence is expected to form a PJTE

intermediate state. In this respect, the STE and DP structures in SiO_2 can both be regarded to result from a specific PTJE interaction.

Consequently we take it for granted that both STEs and DPs occur as a result of a PJTE distortion of that quasi-symmetry configuration. The deviation from symmetry at the saddle-point configuration and the resulting energy inequivalence between STEs and DPs can then be attributed to a static energy term $D/2$ complementary to the vibronic mixing along the reactive coordinate q [7, 11]. Under these conditions the STE-to-DP APES profile should read

$$E_U(q) = 0.5[Kq^2 + \sqrt{(2Gq + D)^2 + E_{gu}^2}]$$
$$E_L(q) = 0.5[Kq^2 - \sqrt{(2Gq + D)^2 + E_{gu}^2}]. \tag{13}$$

Here K is the spring constant, G is the electron–phonon mixing constant and E_{gu} is the energy splitting of the higher-symmetry electronic states. For strong PJTE coupling the lower adiabatic sheet E_L is a double well with minima at q_l and q_r, a peak at q_p and a well inequivalence (zero-point reaction heat) $Q = E_L(q_r) - E_L(q_l)$, which is negative for D positive.

Equation (13) is of the type dealt with by the reaction rate method. It usually incorporates considerable anharmonicity at large $E_{gu} = 2V_{if}$. For this reason use of the quasi-classical techniques (4)–(8) is advised. At the lowest vibronic energy level, equation (3) holds good but now the choice of vibrational frequency therein has to be specified. It may be calculated from the bottom curvature, e.g.

$$\nu_{l/r} = \nu\sqrt{1 - (E_{gu}/4E_{JT})^2}$$

at $D = 0$. Here

$$E_{JT} = G^2/2K$$

is the Jahn–Teller energy.

4. Fitting to the experimental data

From the best fits of equation (1) to the experimental lifetime data we obtained reaction rate parameters for both SiO_2 and Al_2O_3, namely the bare phonon energy $h\nu$, the lattice reorganization energy E_r, the reaction heat Q and the crossover half-splitting V_{if} or, alternatively, the spring constant K, the coupling constant G, the crossover gap energy E_{gu} and the well-inequivalence parameter D. Using equation (13) we could then reconstruct the corresponding APES profiles along the reactive coordinate.

In both cases, summing over discrete energy levels $E_n = h\nu(n + 0.5)$ was carried out. For α-alumina, $h\nu$ was the pertinent phonon quantum, owing to small V_{if}. However, using harmonic energy levels was clearly an oversimplification for α-silica, owing to large E_{gu}, although the estimated bottom anharmonicity amounted to only 5%. For this reason our computed $k_{if}(T)$-values may be an overestimate, introducing some uncertainty in the fitting parameters which is, however, not easy to estimate.

Also, in both cases, the contribution of transitions starting from the lowest vibronic energy level at the STE was evaluated quantum mechanically using equation (3), while transitions from higher levels were dealt with quasi-classically using equations (4)–(6) for alumina and equations (4), (5), (7) and (8) for silica. In the harmonic approximation the integral in (5) has been evaluated analytically [6], which improved considerably

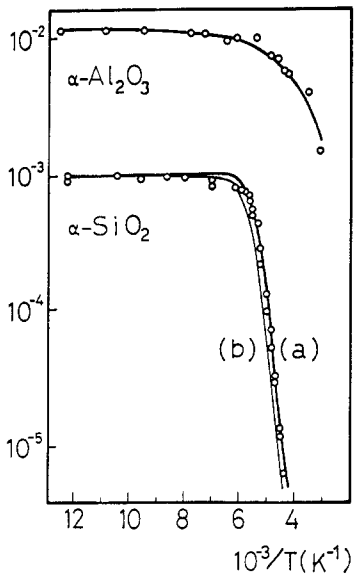

Figure 2. Experimental temperature dependences of the volume change lifetime (○) in α-SiO_2 and α-Al_2O_3 from [2] and from [3], respectively, and reaction-rate best fits (———) using equations (1) and (2). Two options for the reactive-mode vibrator in SiO_2 labelled A and B have been checked, as explained in the text. While the SiO_2 data clearly reveal an adiabatic electron transfer involving strong tunnelling below $T_c/2$ from table 1 and thermally activated tunnelling above that temperature, those for Al_2O_3 point to a non-adiabatic process. Presumably, the low-temperature points yield directly the STE triplet-state radiative lifetime τ_0.

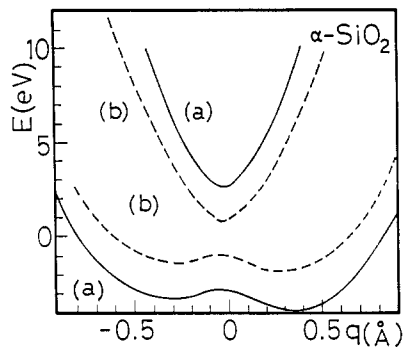

Figure 3. Reconstructed APES profiles in SiO_2 along the mode coordinate q promoting the non-radiative transition. The two options labelled A and B correspond to the two model assumptions for the promoting-mode vibrator, as explained in the text. The upper- and lower-energy sheets represent $E_U(q)$ and $E_L(q)$, respectively, as given by equation (13). The large crossover energy gap indicates an adiabatic behaviour. The parameters used for reconstruction are those listed in table 1. Presumably, a STE-to-DP conversion goes from left to right.

the quality of our calculation for α-alumina. The electron transfer probabilities were calculated using the non-adiabatic form at $2\pi\gamma_n \ll 1$ for alumina or setting them equal to unity for silica.

Our best fits of equation (1) to the experimental data are shown in figure 2. Numerical values of the basic fitting parameters along with certain derivative quantities are listed in table 1 for two values of the parameter E_{gu}, namely 5.5 eV and 2.8 eV. The reconstructed APESS for α-silica for the two sets of fitting parameters are shown in figure 3, curves A and B, respectively. For both cases the fitting parameters are each seen to have very realistic values typical for defect centres in α-quartz [12, 13]. However, fitting may not be expected to be unique when done by five parameters, however reliable. D is the inequivalence factor adopted by Fowler to reconcile asymmetry of the intermediate state and turned out to be nearly 0.5 eV. We found that a negative Q of about 0.5 eV could change the original profile so as to fit the experimental lifetime data. The barrier height of the lowest excited APES between the STE and DP obtained using different parameters agree with each other, indicating that the value is less model dependent.

The fitted oscillator mass in both cases is only several per cent smaller than the respective single-atom vibrator mass. This could arise from the effective character of

Table 1. Fitting reaction rate parameters to lifetime data for SiO_2 ($\tau_0 = 10^{-3}$ s). The two sets of parameters correspond to the two options (figure 3, curves A and B) for the promoting-mode vibrator, mainly composed of a single oxygen or silicon atom, respectively. ν_b is the bare phonon frequency and ν_r the renormalized phonon frequency.

K (eV Å^{-2})	G (eV Å^{-1})	E_{gu} (eV)	D (eV)	M (au)
38.5	15.025	5.5	0.725	15
32	9.67	1.8	0.46	25.67
$h\nu_b$ (eV)	$h\nu_r$ (eV)	E_{JT} (eV)	E_b (eV)	
0.103	0.092	2.932	0.414	
0.072	0.069	1.461	0.412	
E_r (eV)	Q (eV)	T_c (K)	Δq (Å)	$k_{if}(0)$ (s^{-1})
7.176	−0.638	321	0.69	3.75×10^{-9}
4.787	−0.437	425	0.57	5.08×10^{-7}

Table 2. Fitting reaction rate parameters to lifetime data for Al_2O_3 ($\tau_0 = 1.2 \times 10^{-2}$ s).

K (eV Å^{-2})	G (eV Å^{-1})	V_{if} (eV)	M (au)	$h\nu$ (eV)
9.62	2.81	5×10^{-6}	16	0.05
E_r (eV)	Δq (Å)	Q (eV)	E_b (eV)	$k_{if}(0)$ (s^{-1})
1.648	0.59	−0.50	0.20	10.37

the reactive coordinate but it also signifies the physical consistency of the calculation. Indeed, although a two-silicon B_{2u} vibration has been considered likely to produce the distortions at the E_1' centre, the main effect seems to be brought about by a B_{1u}-mode displacement of only one Si atom.

Fitting data for α-Al_2O_3 are presented in table 2. As expected, the bending curvature of the experimental temperature curve, which is much smaller than for α-quartz, arises from a non-adiabatic process involving a very small crossover gap $2V_{if}$. While we cannot at this time judge the physical meaning of the fitting parameters, because of the lack of independent data, the apparent difference between alumina and silica is striking. The reconstructed APES for α-alumina is shown in figure 4.

5. Discussion

For α-SiO_2, the temperature dependence of the STE lifetime has been analysed using the quantum mechanical reaction rate theory and the PJTE conjecture. Fitting to the experimental data can be considered good. Thus, while the particular set of numerical values

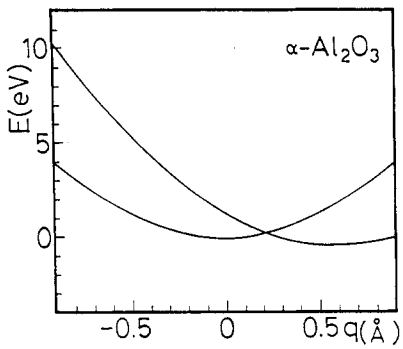

Figure 4. Reconstructed APES profile in α-Al_2O_3 along the mode coordinate q promoting the non-radiative transition. The numerical parameters used for reconstruction are listed in table 2. Now the crossover energy splitting is only 0.01 meV which indicates a non-adiabatic behaviour.

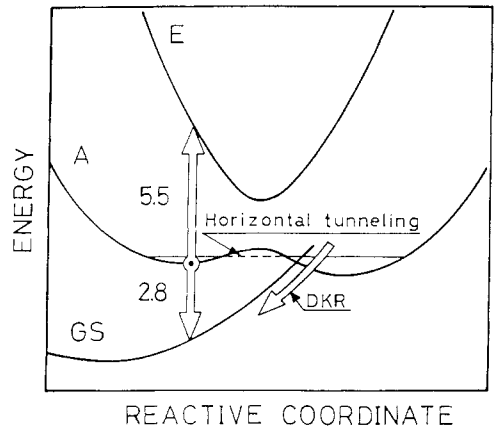

Figure 5. APESs associated with the STE-to-DP conversion (lower adiabatic state) (A), the upper adiabatic state (E) and the electron–hole GS. Presumably, optical transitions from A to E lead to the transient absorption near 5.5 eV, while those from A to GS give rise to the 2.8 eV luminescence. The competing non-radiative process (STE-to-DP transformation) is barrier controlled along A but is short circuited by an effective DKR de-excitation to the GS, thereby preventing the formation of stable DPS in α-quartz.

is not of primary concern for the present discussion, we shall rather emphasize that some of them are model independent within certain ranges. Accordingly, we first discuss the basic model-independent conclusions to be drawn from the analysis of the preceding section.

One of the characteristic features derived from the temperature dependence of the α-SiO_2 lifetime is that numerically E_{gu} greatly exceeds the phonon energy $h\nu$. Consequently, the non-radiative transition from a STE is highly adiabatic and is also strongly coupled to the reactive mode [5, 6], irrespective of the particular model for the saddle-point configuration. It follows that the lowest-state APES exhibits another minimum, which can be ascribed to the DP, besides that pertaining to the STE. As seen in table 1, the values of most parameters show only a weak dependence on the model, except for E_{gu} and $k_{if}(0)$. While the former depends crucially on the model, the latter depends on the APES shape.

The result for α-Al_2O_3 differs substantially from that for α-SiO_2, the value of $2V_{if}$ ($= E_{gu}$) being much smaller. We interpret this to mean that either the electronic states pertaining to the STE and DP are decoupled strongly or that there is a direct crossover between the STE and GS. In the latter case the fitting value of Q may be too small.

While we still do not have a comprehensive understanding of the STE-to-DP transformation in silicon dioxide, the negative reaction heat Q being given by the difference between the static electron and the lattice relaxation energies, it is suggested that the STE-to-DP associated lattice relaxation energy E_r offsets by at least 0.5 eV the increase in Coulomb energy due to dissociation of the pair. This energy offset lowers the interwell barrier from 0.7 to 0.4 eV, increasing the defect formation rate. However, the zero-point rate $k_0 = 5 \times 10^{-7}\ s^{-1}$ is much too low to compete with the radiative lifetime. Now,

since no stable defect production has been observed by electron beam irradiation of α-quartz, it seems likely that the system may de-excite to the GS rapidly after the transformation from STE to DP, perhaps during lattice relaxation following the crossover, as suggested in figure 5. That the APES–GS crossover should have occurred before the equilibrium configuration at DP has been reached is clear, since otherwise radiative DP-to-GS transitions which have not been observed will become likely. Instead, the non-radiative leak of equilibrium DPS is limited in amorphous silica, where relatively stable defect formation is thereby possible. This also emphasizes the peculiar behaviour of silica glass in that the DP–GS crossover now occurs after the equilibrium DP configuration. In any event, attributing the amorphous-to-crystalline difference to differences in the APES–GS crossover is very plausible, since the GS adiabatic potential is expected to vary due to spring constant variations [14]. At the same time, direct STE-to-GS non-radiative de-excitation in α-quartz seems less likely in view of the non-adiabatic electron transfer probability associated with a weakly coupled process [6]. In fact, the STE-associated high luminescent efficiency (about 10%) suggests that the STE–GS crossover energy gap may be too narrow to lead to any adiabatic non-radiative de-excitation, such as observed in α-quartz. The relatively low quantum yield of the luminescence in amorphous silica suggests that the crossing between the lowest excited state and the GS occurs even near the STE configuration.

One way or the other, if the STE-to-DP barrier-controlled process is indeed rate determining, as is at present assumed, the DP-to-GS de-excitation must be much faster. We suggest that the latter step could materialize as a Dexter–Klick–Russell (DKR) overbarrier de-excitation [15], which would be effective unless the DP–GS crossover energy was higher than the STE–DP barrier top. The alternative disposition is eventually materialized in amorphous silica where a slow DP-to-GS leak is controlled by a higher crossover barrier. The virtual non-observation of any radiative DP-to-GS step may now follow if that step is either too slow or has a low energy. Our DKR-based suggestion thus calls for more elaborate theoretical studies of de-excitation paths in particular systems.

Turning next to the associated optical energies, we compute a maximum spring constant of about 15 eV Å^{-2} for an APES–GS crossover to occur near the DP minimum (see figure 5), if the radiative transition energy is held fixed at 2.8 eV. This estimate can be considered realistic, since the GS curvature will be determined by a small-reduced-mass vibrator involving the motion of more than two atoms. At the same time, the unique APES curvature at either well is larger by a factor of at least 2. Optical transitions from the lower- to the higher-branch APES at the STE well should correspond to the observed transient absorption band in α-quartz peaked at about 5.5 eV. In agreement, we at present estimate an absorption peak at about 5.85 eV, from the underlying Jahn–Teller energy. In amorphous silica, optical absorptions attributed to STES and DPS have each been identified [16]. They occur at 5.4 eV and 5.8 eV, respectively, again in accord with the Jahn–Teller energy, as calculated for the crystalline case. The optical absorption predicted from our first set of fitting parameters in table 1 peaks at about 12 eV. Without an adequate knowledge of the saddle-point configuration, it is premature to discuss the validity of the parameters. We would finally like to comment on the recent observation of an optically induced DP-to-STE back process through pumping in the DP-associated absorption band of amorphous silica [17]. This optical transfer is easily understandable as a lift-off to the upper APES followed by de-excitation to the STE well. However, it is not immediately clear just how that de-excitation energy splits into non-radiative and radiative components, since the latter have not been identified as yet.

The nature of the APES for Al_2O_3 is less clear, partly owing to the lack of experimental information; neither luminescence nor optical absorption bands have been assigned,

but it is only the transient volume change that has been measured. According to our fitting, the optical absorption energy of the STE is evaluated to be 1.64 eV. The search for a transient optical absorption has been carried out down to 0.8 eV. Thus, if STEs similar to those in SiO_2 are generated, the optical absorption energy should lie below 0.8 eV. In this case, we do not expect any large Stokes shift, and hence the luminescence energy will be in the vacuum UV, where no transient optical absorption measurements have been carried out. Further work is necessary to elucidate the nature of the STEs in Al_2O_3.

6. Conclusion

We believe that we have demonstrated that applying a quantum mechanical non-radiative rate theory to process experimental lifetime data can give us some information about the APESs involved, and in any event much more than the simple classical analysis can. In particular, assuming that the radiationless de-excitation path in α-quartz is simply that which also leads to the dissociation of STEs into DPs, we show the feasibility of a vibronic mixing model in which the STEs and DPs both result from the breaking of a higher-symmetry configuration involving a nearby vacancy–interstitial pair in the oxygen sublattice. An APES is thus obtained controlling the STE-to-DP transformation, which appears to be short circuited by a rapid DKR de-excitation to the electron–hole GS so that no stable DPs form in crystalline SiO_2. Presumably, mainly owing to the structural dependence of the GS-associated spring constant, the DKR pathway is hindered through an increase in the crossover barrier in amorphous SiO_2 which results in stable DPs. In this way the defect-related features of both materials may be explained simply and from a common viewpoint. Further theoretical and experimental research may use the present conjectures as a working hypothesis. Apparently the alumina case needs more study.

This work is a part of a broader theoretical study of STEs and DPs in α-quartz, to appear elsewhere [10, 18].

Acknowledgments

It is a pleasure acknowledging useful discussions with Dr K Tanimura, Dr C Itoh, Dr A Shluger and Dr J Valbis.

References

[1] Itoh N and Tanimura K 1986 *Radiat. Eff.* **98** 435
Hayes W 1986 *J. Lumin.* **31–2** 99
Hayes W, Kane M J, Salminen O, Wood R L and Doherty S P 1984 *J. Phys. C: Solid State Phys.* **17** 2943
[2] Tanimura K, Tanaka T and Itoh N 1983 *Phys. Rev. Lett.* **51** 423
Tanimura K, Tanaka T and Itoh N 1984 *Nucl. Instrum. Methods* B **1** 187
[3] Itoh C, Tanimura K and Itoh N 1986 *J. Phys. C: Solid State Phys.* **19** 6887
[4] Itoh N 1985 *Cryst. Latt. Defects Amorph. Mater.* **12** 103
[5] Christov S G 1980 *Collision Theory and Statistical Theory of Chemical Reactions* (Berlin: Springer)
[6] Christov S G 1984 *Phil. Mag.* B **49** 325
Christov S G 1985 *Phil. Mag.* B **52** 71, 91
Georgiev M 1985 *J. Informat. Record. Mater.* **13** 75, 177, 245
Georgiev M 1985 *Rev. Mexicana Fis.* **31** 221

[7] Georgiev M and Manov A 1988 *Czech. J. Phys.* B **38** 83
[8] Leung C H, Brunet G and Song K S 1985 *J. Phys. C: Solid State Phys.* **18** 4459
Song K S, Leung C H and Williams R T 1989 *J. Phys.: Condens. Matter* **1** 683
[9] Shluger A L 1988 *J. Phys. C: Solid State Phys.* **21** L431
[10] Shluger A and Stefanovich E 1990 *Phys. Rev.* B at press
[11] Edwards A H, Beall Fowler W and Feigl F J 1988 *Phys. Rev.* B **37** 9000
[12] Yip K L and Beall Fowler W 1974 *Phys. Rev.* B **11** 2327
[13] Fowler W B 1982 *Radiat. Eff.* **64** 63; 1983 *Radiat. Eff.* **72** 27
[14] The suggestion that the GS APES is influenced by the local structure of the amorphous material is based on the experimental observation that the luminescence undergoes a blue shift as the delay time is increased, while no shift is observed in the optical absorption from the initial state of that luminescence. This suggestion is consistent with the result that the luminescence bands in crystalline and amorphous SiO_2 differ appreciably but the optical absorption bands do not. Thus the reactive (defect formation) APES is not likely to undergo major changes from crystalline to amorphous.
[15] Stoneham A M and Bartram R H 1978 *Solid-State Electron.* **21** 1325
[16] Griscom D L 1979 *Proc. 33rd Frequency Control Symp.* (Washington, DC: Electronic Industries Association) p 98
[17] Itoh C, Suzuki T and Itoh N 1990 *Phys. Rev.* B **41** 3794
[18] Shluger A, Georgiev M and Itoh N 1990 *Phil. Mag.* at press